MOLECULAR AND CELLULAR BIOLOGY, June 2008, p. 3776–3789 Vol. 28, No. 11
0270-7306/08/$08.00+0 doi:10.1128/MCB.00507-07


# αPIX Rho GTPase Guanine Nucleotide Exchange Factor Regulates Lymphocyte Functions and Antigen Receptor Signaling▽

Karine Missy,[1]† Bin Hu,[1]† Kerstin Schilling,[1,2] Anke Harenberg,[1] Vadim Sakk,[1] Kerstin Kuchenbecker,[3] Kerstin Kutsche,[3] and Klaus-Dieter Fischer[2]*

*Institute of Physiological Chemistry, University of Ulm, Albert-Einstein-Allee 11, 89081 Ulm, Germany[1]; Institute of Biochemistry and Cell Biology, Otto von Guericke University, Leipziger Str. 44, 39120 Magdeburg, Germany[2]; and Institute of Human Genetics, University Medical Center Hamburg-Eppendorf, Butenfeld 42, 22529 Hamburg, Germany[3]*

Received 22 March 2007/Returned for modification 30 April 2007/Accepted 17 March 2008

**αPIX is a Rho GTPase guanine nucleotide exchange factor domain-containing signaling protein that associates with other proteins involved in cytoskeletal-membrane complexes. It has been shown that PIX proteins play roles in some immune cells, including neutrophils and T cells. In this study, we report the immune system phenotype of αPIX knockout mice. We extended αPIX expression experiments and found that whereas αPIX was specific to immune cells, its homolog βPIX was expressed in a wider range of cells. Mice lacking αPIX had reduced numbers of mature lymphocytes and defective immune responses. Antigen receptor-directed proliferation of αPIX$^-$ T and B cells was also reduced, but basal migration was enhanced. Accompanying these defects, formation of T-cell–B-cell conjugates and recruitment of PAK and Lfa-1 integrin to the immune synapse were impaired in the absence of αPIX. Proximal antigen receptor signaling was largely unaffected, with the exception of reduced phosphorylation of PAK and expression of GIT2 in both T cells and B cells. These results reveal specific roles for αPIX in the immune system and suggest that redundancy with βPIX precludes a more severe immune phenotype.**

The activation of lymphocytes by antigen is critical to the generation of specific immune responses. An antigen stimulates signaling cascades in T and B cells via the T-cell antigen receptor (TCR) and the B-cell antigen receptor (BCR). These signaling cascades produce multiple measurable outputs, including tyrosine phosphorylation of proteins, mitogen-activated protein kinase activation, calcium fluxing, and protein degradation. On a larger scale, activation of signaling causes remodeling of macromolecular complexes, such as immune synapses or focal adhesions, enabling a cell to differentiate or to migrate (6, 46). One family of proteins that is important for organizing such signaling complexes in immune cells is the Rho GTPase guanine nucleotide exchange factors (RhoGEFs) (21, 55). RhoGEFs are associated with cytoskeletal remodeling, since they are enzymes that activate Rho family GTPases, such as Rho, Rac, or Cdc42, by catalyzing the exchange of GTP for GDP on the GTPase (26). RhoGEFs contain multiple protein interaction domains and bind to a variety of signaling proteins. The PIX (*p*21-*i*nteracting e*x*change factor) family RhoGEFs were identified through binding to the PAK kinases (serine/threonine p21-activated kinases) (2, 34, 50).

Members of the PIX family of GEFs include αPIX/Cool-2 (*c*loned *o*ut *o*f *l*ibrary), βPIX/Cool-1/p85SPR, and an alternate isoform of βPIX called p50$^{cool-1}$ (2, 34, 40). PIX proteins have in common an SH3 domain, a paired *Dbl* homology (DH) domain, and a pleckstrin homology (PH) domain for activation of Rho GTPases (also known as a RhoGEF domain), but they differ in the lengths of their N- and C-terminal regions (15, 30): αPIX contains an N-terminal calponin homology (CH) domain (51), while βPIX does not. Also, the αPIX gene, but not the βPIX gene, maps to the X chromosome (32). Both PIX proteins share a coiled-coiled domain implicated in dimerization and a domain called the GIT-binding sequence (50). Although PIX GEFs can activate Rac1 and Cdc42 GTPases, they are subject to many levels of control, including requirements for phosphorylation (54), for monomerization or dimerization (16), for relief from an inhibitory domain (15), and for binding to activated GTPases (3).

PIX proteins associate with a wide variety of proteins, from the neuronal synapse protein Shank (41) and the polarity complex protein Scribble (1), to signaling proteins such as PAK or phosphatidylinositol 3-kinase (p85 subunit) (34, 60), to actin-associated proteins such as β-parvin/affixin (49) and Abi-1 (12). PIX proteins also bind to degradation-related proteins, such as E3 ubiquitin ligases c-Cbl (18) and atrophin-interacting protein 4 (28), and calpain regulatory subunit (48). PIX proteins may play roles in lymphocyte disease by facilitating human immunodeficiency virus Nef functions (9) and through binding to X-linked lymphoproliferative disease protein SAP (23). The predominant binding partners for PIX proteins, however, are GIT proteins (G-protein-coupled receptor kinase-interacting proteins 1 and 2), also known as CAT proteins/p95PKL/APP1/2 (25). PIX proteins and GIT proteins associate in large, stable oligomeric complexes that recruit Rac1 and Cdc42 GTPases and PAK kinases (45). These associations enable PIX protein participation in actin-dependent cell functions, such as migration (57), cell spreading (48), neurite extension (53, 61), and focal complexes (50). It is likely that these functions are tightly coordinated with those of GIT proteins, which include membrane recycling and endosomal dynamics (25).

* Corresponding author. Mailing address: Institute of Biochemistry, Otto von Guericke University, Leipziger Str. 44, 39120 Magdeburg, Germany. Phone: 49-391-671-4288. Fax: 49-391-671-5898. E-mail: klaus.fischer@med.ovgu.de.

† K.M. and B.H. contributed equally to this work.

▽ Published ahead of print on 31 March 2008.

The mutation of αPIX in mice results in neutrophils defective in orienting and migrating toward a chemoattractant (33). This phenotype resembles that of GIT2 knockout mice, which also have neutrophils with direction-sensing defects (36). In humans, αPIX mutations are associated with X-linked mental retardation (32). αPIX knockout lymphocytes have not been described in detail; however, results of studies on PIX in Jurkat T cells point to multiple roles for PIX proteins in T cells. Using overexpression of a mutant βPIX to block PIX signaling in Jurkat T cells, it was shown that PIX proteins are complexed with GIT and PAK and are required for PAK activation by TCR (31). A subsequent study revealed that PIX proteins target PAK to the immune synapse and are required for TCR signaling to phospholipase C-γ1 and transcription (43). As the overexpression of a βPIX mutant would likely block αPIX signaling as well, the functions that can be specifically ascribed to αPIX in T cells have not yet been determined.

We aimed to investigate αPIX alone, and not βPIX, in lymphocytes. To this end, we generated αPIX-deficient mice by gene targeting. We describe here several cellular and molecular defects that can be specifically attributed to αPIX. On a systemic level, immune responses were defective and mature lymphocyte populations were reduced. At the cellular level, antigen receptor-induced proliferation was decreased and spontaneous migration was increased in the absence of αPIX. Molecular events that were altered in αPIX$^-$ T and B cells included decreased GIT2 expression, PAK phosphorylation, and recruitment of PAK and Lfa-1 to the immune synapse. Thus, this study of αPIX$^-$ mice identifies nonredundant roles for αPIX that cannot be compensated for by βPIX and reveals new functions for RhoGEFs in the immune system.

## MATERIALS AND METHODS

**αPIX gene targeting.** A genomic mouse 129/Ola library (RZPD Center, Berlin, Germany) was screened with an α*PIX* cDNA probe amplified by reverse transcription-PCR. Cosmids were isolated, and a portion of the genomic DNA of one of these cosmids (clone MPMGc121F09630) was subcloned into pBluescript and used to generate the targeting vector. Genomic DNA encoding amino acids 400 to 465 was exchanged by a neomycin cassette flanked by *loxP* sites. The targeting construct was linearized and electroporated into E14 (129/Ola) embryonic stem (ES) cells. Homologous recombinants were analyzed by Southern blotting and PCR. Targeted ES clones were aggregated with eight-cell-stage embryos (39), which were subsequently transferred to pseudopregnant mice to generate chimeric offspring. Chimeric males were then bred with C57BL/6 females to obtain αPIX knockout mice. OT-II mice were kindly provided by F. R. Carbone. Mice used in this study were backcrossed to C57BL6 mice for four to five generations, and 6- to 12-week-old littermates or age-matched mice were analyzed. Animals were housed under specific-pathogen-free conditions under institutional guidelines.

**Flow cytometry, cell purification, proliferation, and migration.** Thymuses, spleens, and lymph nodes were dissected and crushed in RPMI medium, and samples were depleted of red blood cells. Cell surface marker expression was analyzed using a four-color flow cytometer (FACScalibur; Becton Dickinson) and CellQuest software. The following antibodies were used: CD21-fluorescein isothiocyanate (FITC), CD23-phycoerythrin (PE), B220-peridinin-chlorophyll-protein complex (PerCP), Thy1.2-allophycocyanin (APC), CD4-PE, CD8α-FITC, CD8α-PE, B220-FITC, immunoglobulin M (IgM)-PE, B220-Cy5, IgD-FITC, and IgM-FITC (Pharmingen). Cell analysis was performed by complement lysis purification and fluorescence-activated cell sorting (FACS) as previously described (21, 55). In brief, B cells were purified from mouse spleens by complement lysis of cells precoated with anti-CD4 (no. 172) and anti-CD8 (31 M) followed by gradient purification over Lympholyte M (Cedarlane). T cells were purified in the same manner, except splenocytes were precoated with anti-B220 (RA3-3A1) and anti-major histocompatibility complex II (MHC-II; anti-IAb, IAd hybridoma; ATCC HB-35). Cell purity was assessed by flow cytometry. Purified (>90%) B cells ($1 \times 10^5$) were seeded into round-bottom 96-well plates (Costar) in freshly prepared Iscove's modified Dulbecco's medium, 10% fetal calf serum, and $10^{-5}$ M β-mercaptoethanol or RPMI and activated with B7.6 monoclonal antibody (MAb) anti-IgM, F(ab′)2 anti-IgM (Jackson Laboratories), anti-CD40 [FGK45(47)], interleukin-4 (IL-4), or lipopolysaccharide (LPS). B cells were harvested at 3 days after a 12-h pulse with 0.5 to 1 μCi [$^3$H]thymidine/well. Purified lymph node T cells ($1 \times 10^5$/well) were stimulated with anti-CD3 alone (2.5 μg/ml; MAb 145-2C11) or together with anti-CD28 (0.5 μg/ml; MAb 37.51; Pharmingen) and concanavalin A (ConA; 5 μg/ml), or with a combination of phorbol myristate acetate (PMA; 5 ng/ml) plus ionomycin (0.5 μg/ml; Sigma). Supernatants were collected for cytokine enzyme-linked immunosorbent assays (ELISAs) before [$^3$H]thymidine for proliferation assays was added. To assay migration, Lympholyte M-purified splenocytes or lymph node cells ($1 \times 10^6$) were incubated at 37°C for 0.5 h in RPMI containing 0.25% fatty acid-free bovine serum albumin (Sigma) and 10 mM HEPES. Transmigration to SDF/1α (R&D) was assayed in 5-μm-pore-size Costar transwell plates. Cells were stained with anti-CD4–FITC, anti-CD8–PE, and anti-B220–PerCP and counted by FACS. Migration was calculated as the percentage of the "input" samples.

**Cell signaling and αPIX expression.** For analysis of αPIX expression, tissues and hematopoietic cells (purity, >90%) from wild-type mice were isolated and purified as previously described (21). Protein content was estimated by a Bradford assay (Bio-Rad, Richmond, CA), and equal amounts of protein (70 μg) from each lysate were used to determine PIX expression. Proteins were resolved by sodium dodecyl sulfate-polyacrylamide gel electrophoresis (SDS-PAGE) and analyzed with an anti-PIX antibody recognizing both α- and βPIX as described previously (34) or commercially obtained (Chemicon International, Temecula, CA) with similar results. To analyze lymphocyte signaling, purified T cells were preincubated for 1 h at 37°C in RPMI and then incubated with 15 μg/ml anti-CD3 alone or in combination with 5 μg/ml anti-CD28 for 10 min on ice. Cells were warmed at 37°C for 1 min, and stimulations were started by the addition of 30 μg/ml anti-hamster antibody (Serotec). B-cell stimulation was performed using anti-CD40 (FGK 45) (47) as described elsewhere (55). Immunoblot assays were performed with anti-phospho-PAK1/2 (Ser199/204 of PAK1 and Ser192/197 of PAK2; Cell Signaling), anti-phospho-Erk1/2 (E4; Santa Cruz), anti-phospho-c-Cbl (Y774; Cell Signaling), and anti-PAKα (N20; Santa Cruz), anti-GIT1 (H-170; Santa Cruz sc-1396), anti-GIT1/2 (p95PKL/GIT; BD 611388), anti-SAP (Chemicon AB4069), and anti-Cbl (Santa Cruz sc-170). Equal loading of membranes was confirmed by Erk1/2 (K-23; Santa Cruz) staining. GTPase activity assays using glutathione *S*-transferase–PAK as activation probe and anti-Rac1 (Santa Cruz) and anti-CDC42 antibodies (Transduction Laboratories) were performed as described elsewhere (24). To measure calcium fluxing, lymph node or splenic cells ($5 \times 10^6$) were incubated with 4 μg/ml of Fluo-3-AM per ml and 10 μg/ml of FuraRed (Molecular Probes) in RPMI for 45 min at 37°C. T cells were stained with anti-Thy1–APC (Pharmingen) on ice and stimulated with anti-CD3 (5 μg/ml) cross-linked with anti-hamster IgG (10 μg/ml) to start stimulation. B cells were stained with anti-B220 (Pharmingen) on ice and stimulated with F(ab′)2 anti-IgM (10 μg/ml). Calcium influx was monitored by flow cytometry, and data were analyzed with FlowJo software. TCR-induced actin polymerization using anti-CD3 at 5 μg/ml, followed by anti-hamster IgG at 5 μg/ml, was performed essentially as described previously (17).

**GIT2 expression analysis.** Quantitative reverse transcription-PCR was performed as described elsewhere (10). In brief, total RNA isolated from mouse lymph node T cells using the High Pure RNA isolation kit (Roche Diagnostics) was used to prepare random-primed cDNA. Quantitative PCR was conducted using the QuantiTect Sybr green PCR kit (Qiagen). The real-time PCR was performed in a Light Cycler (Roche) using Light Cycler software (Roche) for fluorescence detection and data evaluation. The housekeeping gene PBGD was used to standardize the cDNA content. The following GIT2 oligonucleotide primers were used: 5′-AACACTCTCTGCTGGACCCT-3′ and 5′-GGACGAA CGCTAACATCTGA-3′ (N-terminal primer) and 5′-CAGGAGACTCCAGCT TACCG-3′ and 5′-CATAGGCACACTGGATGACC-3′ (C-terminal primer). For Northern blot analysis, total RNA from lymph nodes was separated by gel electrophoresis, blotted, and probed with an N-terminal GIT2 probe generated by reverse transcription-PCR using the following oligonucleotide primers: 5′-C CTGCTCCAGATGGTTGAGA-3′ and 5′-CGCCTGTCAACTTCGTCGTA-3′. Specific protein expression was analyzed by Western blotting using an antibody recognizing GIT2 long and GIT2 short (Becton-Dickinson).

**T-cell–APC conjugate formation and synapse microscopy.** For peptide-induced cell-cell conjugation, LB27.4 cells (*H-2$^{d/b}$*-restricted B-cell hybrid; ATCC) were pulsed with 1 μg/ml OVA II peptide ($OVA_{329–339}$) at 37°C for 4 h and stained with 5 μM CellTracker Orange 5 (and 6)-{[(4-chloromethyl)benzoyl]amino}tetramethylrhodamine (CMTMR). Purified OT-II TCR-transgenic CD4$^+$ T cells were

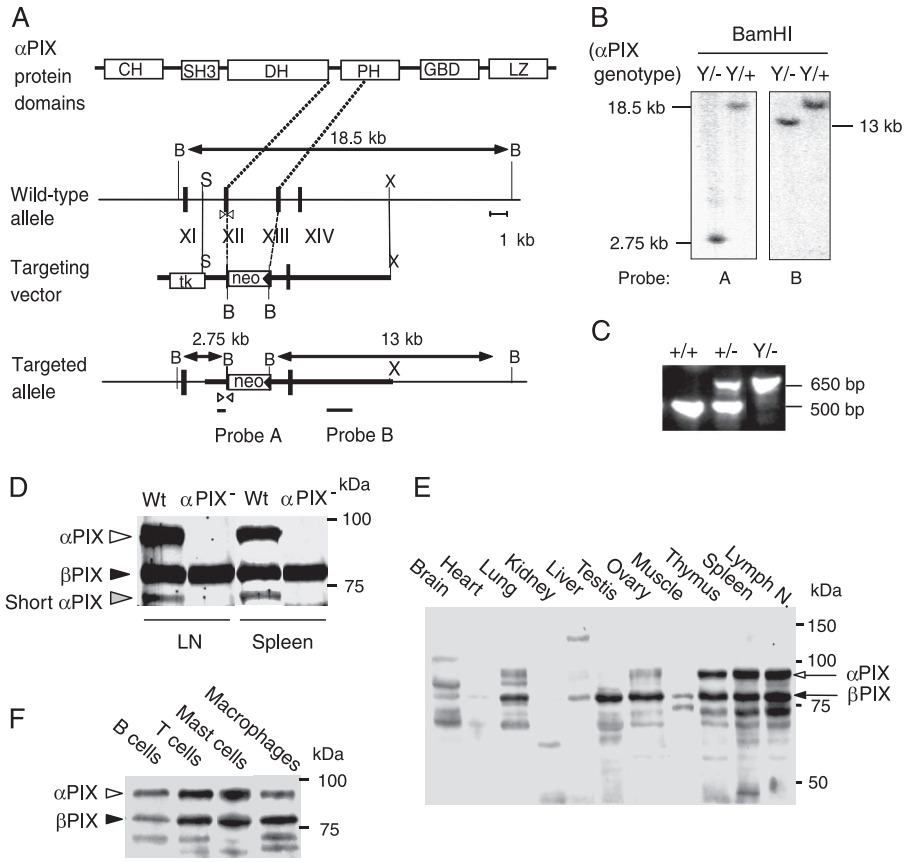


FIG. 1. Generation of αPIX⁻ mice. (A) Schematic representation of the domains of αPIX, the *apix* genomic locus, the targeting vector, and the targeted allele. Domains are indicated by open boxes, exons XI to XIV are represented by solid boxes, and locations of primers used for PCR are shown as arrowheads. A segment of the PH domain was replaced with the neomycin resistance cassette (neo) flanked with BamHI sites, with the direction of transcription indicated by an arrowhead. Predicted sizes of fragments generated by digestion with BamHI are shown. Probes A and B were used for Southern blot detection of short and long arms, respectively. B, BamHI; S, SacI; X, XbaI. (B) Southern blot analysis of genomic DNA from wild-type (Y/+) and hemizygous (Y/−) αPIX-deficient ES cell clones. Genomic DNA was digested with BamHI and hybridized with probe A or probe B. (C) PCR was performed to analyze littermates derived from crosses between αPIX heterozygous females (+/−) and wild-type males (Y/+). DNA fragments derived from wild-type (500-bp) and targeted (650-bp) alleles are indicated. (D) Immunoblot analysis of lymph node (LN) and spleen whole-cell lysates prepared from wild-type (Wt) and αPIX⁻ mice using an anti-PIX antibody. α- and βPIX isoforms are indicated. (E) Expression of αPIX in hematopoietic cells. Cell homogenates from the indicated tissues were resolved by SDS-PAGE and immunoblotted with a polyclonal anti-PIX antibody. (F) Hematopoietic cells were purified and analyzed as for panel E.

stained with 0.1 μM 5 (and 6)-carboxyfluorescein diacetate succinimidyl ester (CFSE), mixed with B cells at a 1:1 ratio, and centrifuged at 40 × *g* for 5 min to initiate conjugate formation and then incubated at 37°C for 30 min. Resulting conjugates were analyzed by FACS. To assess immune synapses, purified C57BL/6 wild-type splenic B cells were pulsed overnight at 37°C with OVA II peptide (10 μg/ml) in the presence of LPS (30 μg/ml). Cells were collected, stained with CellTracker Blue 7-amino-4-chloromethylcoumarin (CMAC; (Molecular Probes), and mixed at a 1:1 ratio with purified $CD4^+$ OT-II $CD4^+$ T cells from lymph nodes. The mixed cell suspension was briefly centrifuged (30 seconds at 4,500 × *g*) to initiate conjugation. After incubation at 37°C for 5 min, cells were carefully resuspended, settled on an eight-well mask slide, and fixed with 4% paraformaldehyde. Fixed cells were permeabilized with 0.1% Triton X-100 and stained with Alexa 488-conjugated anti-CD3ε (145-2C11; Pharmingen) and either anti-PIX (Chemicon), anti-PAK2 (Cell Signaling), or anti-phospho-PAK1/2 (PAK1 S199/S204, PAK2 S192/S197; Cell Signaling) followed by Alexa 594-conjugated goat anti-rabbit IgG (Molecular Probes) as a secondary antibody. To observe integrin clustering in synapses, the mixed cells were incubated at 37°C for 30 min and then allowed to settle on the slide, fixed, permeabilized, and stained with biotinylated anti-mouse CD11a (αL, LFA-1 α chain; BD) and Cy3-conjugated streptavidin. Slides were observed with both a conventional Leica DM IRB/E microscope (Leica Microsystems Wetzlar GmbH, Germany) and Openlab software (Improvision) for quantification experiments and a Zeiss Axiovert 200 M microscope equipped with an Apotome device (Carl Zeiss, Germany) to produce images with a similar quality as those produced by confocal microscopy.

**Immunizations.** Mice were immunized by intraperitoneal injection of 100 μg TNP-keyhole limpet hemocyanin (KLH) or 10 μg trinitrophenyl (TNP)-Ficoll, respectively. TNP-KLH mice were boosted 14 days after the first injection. Sera were collected before immunization and on days 7 and 14 after TNP-Ficoll immunization or on days 14 and 21 after TNP-KLH immunization. Immunoglobulins were detected by alkaline phosphatase-conjugated antibodies to mouse IgG1, IgG2a, and IgG3 and biotinylated antibody to mouse IgM (all from Pharmingen) by ELISA. The amount of each antigen-specific isotype was determined by comparing test samples to a standard serum pooled from immunized wild-type and αPIX-deficient mice (21).

## RESULTS

**Generation of αPIX knockout mice.** To investigate αPIX functions in the immune system in vivo, we generated a null mutation of the mouse *apix* locus (Fig. 1A). Correct integration of the targeting vector was identified by Southern blotting using the indicated 5′ and 3′ probes (Fig. 1B). As the αPIX locus is located on the X chromosome and the ES cells used for

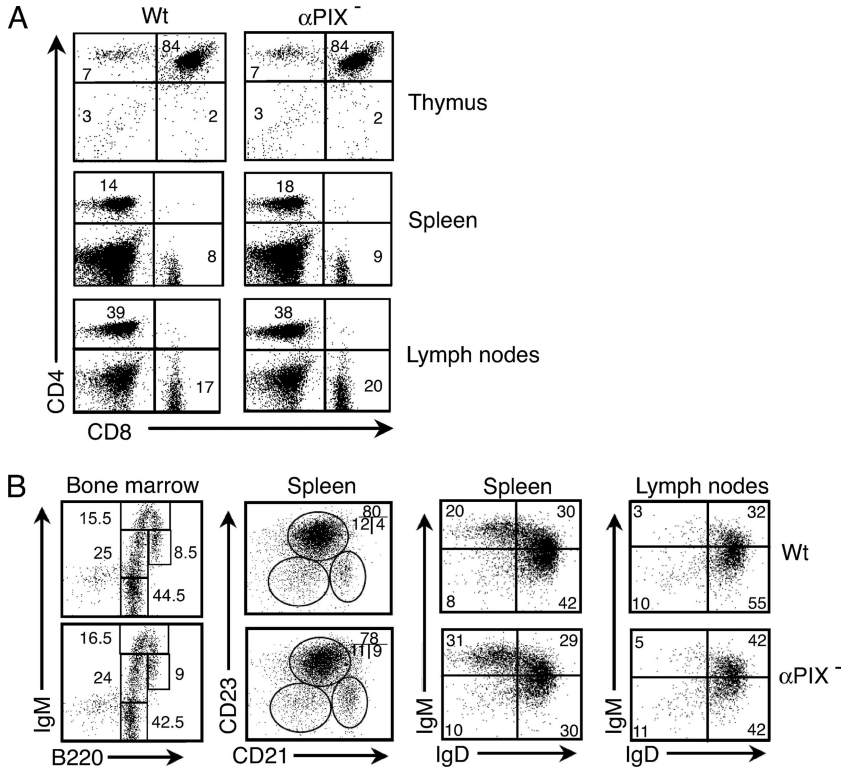


FIG. 2. Analysis of lymphocyte populations in αPIX⁻ mice. (A) T-cell development in normal (Wt) and αPIX⁻ mice. Thymocytes and splenic and lymph node T cells from 6- to 8-week-old wild-type and αPIX⁻ littermates were stained with anti-CD4–PE and anti-CD8–FITC and analyzed by FACS. Percentages of cells within the lymphocyte populations are indicated in the relevant quadrants. (B) B-cell development alterations in αPIX⁻ mice. Bone marrow B-cell precursors (left panel), splenic B cells (middle two panels), and lymph node B cells (right panel) from 8- to 10-week-old wild-type and αPIX⁻ littermates were analyzed by FACS following staining with anti-B220–FITC and anti-IgM–PE (bone marrow), anti-B220–PerCP, anti-IgM–PE and anti-IgD–FITC (spleen and lymph nodes), and anti-B220–PerCP, CD21-FITC, and CD23-PE (spleen). Percentages of cells within the lymphocyte population are indicated in the relevant quadrants.

homologous recombination were obtained from a male (XY), targeted clones did not contain the wild-type allele. Male αPIX mutant mice were null for αPIX, while female mice could be either heterozygous or homozygous for the mutation. Mice generated from ES cells were genotyped by PCR (Fig. 1C). Mice carrying the targeted αPIX allele did not express αPIX protein (Fig. 1D). In the analyses presented here, we did not use heterozygous αPIX mice as experimental controls because X chromosome inactivation would lead to αPIX being inactivated in some cells and tissues, possibly resulting in αPIX⁻ cells as controls. Rather, strain- and age-matched mice that were wild type for αPIX were used as controls. The αPIX mutant mice referred to here are described as αPIX⁻ regardless of gender and were born at Mendelian frequencies, were fertile, and did not exhibit any obvious physical abnormalities.

**αPIX expression primarily in immune cells.** It is known that PIX proteins are widely expressed (34). To address the question of PIX expression in more depth, we used a polyclonal antibody directed against the SH3-DH-PH domains of αPIX to probe protein extracts from a wide range of tissues and cells. This antibody recognized both αPIX and βPIX (34), allowing us to compare the expression profiles of both proteins. Whereas βPIX expression was detected in most tissue types tested, including lung, testis, ovary, and lymph nodes, αPIX expression was mainly restricted to hematopoietic tissues (thymus, spleen, and lymph nodes) (Fig. 1E). Additional examination of hematopoietic cells showed that αPIX was expressed in B cells, T cells, cultured bone marrow-derived mast cells, and to a lesser extent in bone marrow-derived macrophages (Fig. 1F). We also observed that on the immunoblots for αPIX a second protein of about 65 kDa was missing in αPIX-deficient cells, suggesting that a shorter form of αPIX may also be expressed in hematopoietic cells (Fig. 1D). Expression of βPIX was unaffected by the loss of the p95 kDa and the p65 kDa isoforms of αPIX (Fig. 1D). Together, these data show that unlike βPIX, αPIX is mainly expressed in hematopoietic cells and tissues.

**Reduced numbers of mature lymphocytes in αPIX⁻ mice.** The high levels of αPIX expression in lymphoid organs pointed to a role for αPIX in lymphocyte development. Flow cytometry analysis of lymphocyte development in αPIX⁻ mice revealed that immature lymphocytes, including thymocyte subsets ($CD4^+$ $CD8^+$ double-positive immature thymocytes and $CD4^+$ or $CD8^+$ single-positive thymocytes) (Fig. 2A) were normal. Immature bone marrow B-cell subsets ($B220^+$ $IgM^{lo\text{-}hi}$) were also normal (Fig. 2B). However, absolute numbers of mature T and B cells were significantly reduced in peripheral lymphoid organs (Table 1). T cells ($CD4^+$ or $CD8^+$ single positive) in spleen and lymph nodes were present in normal relative numbers but were reduced in overall number by ap-

TABLE 1. Lymphocyte populations in αPIX$^-$ mice

| Tissue ($n$)[b] and cell population | No. of cells ($10^6$)[a] | | $P$ value[d] |
|---|---|---|---|
| | Wild type | αPIX$^-$ | |
| Thymus (10) | | | |
| Total | 129 ± 57.5 | 109 ± 50.3 | |
| CD4$^-$ CD8$^-$ | 3.88 ± 2.3 | 3.95 ± 1.02 | |
| CD4$^+$ CD8$^+$ | 90.4 ± 32.8 | 81.5 ± 24.5 | |
| CD4$^+$ CD8$^-$ | 9.85 ± 5.5 | 8.5 ± 2.98 | |
| CD4$^-$ CD8$^+$ | 3.75 ± 2.6 | 2.97 ± 1.08 | |
| Bone marrow (8) | | | |
| Total | 13.83 ± 2.1 | 13.96 ± 4.94 | |
| B220$^+$ | 0.63 ± 0.3 | 0.44 ± 0.2 | |
| Spleen (9) | | | |
| Total | 71.9 ± 25.8 | 50.4 ± 23.8 | |
| B220$^+$ | 27.9 ± 11 | 22.3 ± 10.7 | |
| CD4$^+$ | 10.06 ± 3.5 | 5.47 ± 2.63 | <0.05 |
| CD8$^+$ | 5.42 ± 2.4 | 3.27 ± 1.35 | <0.05 |
| Lymph nodes (9 or 5)[c] | | | |
| Total | 21 ± 5 | 10.4 ± 2.9 | <0.001 |
| B220$^+$ | 7.6 ± 2.8 | 3.5 ± 1.4 | <0.05 |
| CD4$^+$ | 9.7 ± 0.96 | 4.3 ± 1 | <0.001 |
| CD8$^+$ | 5.5 ± 1.2 | 2.34 ± 0.5 | <0.005 |

[a] Cells from the thymus, bone marrow, spleen, and lymph nodes of wild-type and αPIX$^-$ littermates (6- to 8-weeks old) were counted and stained for the indicated cell surface markers. Cell populations were determined by flow cytometry. Data are means ± standard deviations.

[b] Number of animals evaluated (for each tissue or organ, equal numbers of wild-type and αPIX$^-$ mice were evaluated).

[c] For lymph node evaluations, cells from nine mice of each group were evaluated for total cell counts; B220$^+$, CD4$^+$, and CD8$^+$ counts were based on five animals from each group.

[d] Probability was calculated using Student's $t$ test.

proximately half (Table 1). Similarly, mature B-cell numbers in lymph nodes were reduced by about half (Table 1). B-cell numbers in spleens were reduced, although not significantly, but some subsets were present in abnormal ratios: marginal zone B cells (CD21$^{hi}$ CD23$^{lo}$) in the spleen were increased approximately 1.5- to 2-fold and immature B cells (IgM$^{hi}$ IgD$^{lo}$), which include marginal zone B cells, and transitional B cells (IgM$^{hi}$ IgD$^{hi}$) in spleen were increased, while mature B cells (IgM$^{lo}$ IgD$^{hi}$) were decreased in αPIX$^-$ mice (Fig. 2B). Thus, αPIX is dispensable for development of most subsets of lymphocytes but is required for limiting marginal zone B-cell numbers and for promoting numbers of mature T cells and B cells.

**Reduced immune responses in αPIX$^-$ mice.** B-cell production of antibodies in response to antigen is central to specific immunity. To investigate immune responses in αPIX knockout mice, wild-type and αPIX$^-$ mice were immunized with the thymus-dependent antigen TNP-KLH and with the thymus-independent type 2 antigen TNP-Ficoll, and the resulting levels of specific blood serum antibodies were analyzed. αPIX-deficient mice immunized with TNP-KLH produced significantly less antibodies at 14 and 21 days postimmunization. αPIX$^-$ mice immunized with TNP-Ficoll also produced significantly lower antibodies, with reduced IgM at 7 and 14 days postimmunization and reduced IgG3 at 7 days (Fig. 3). These results demonstrate global defects in antibody production in αPIX$^-$ mice, including a defect in IgM production that was not alleviated by the increased numbers of MZ B cells, the cells that normally direct T-cell-independent immune responses (4). The defective αPIX$^-$ immune responses may reflect a role for αPIX in T helper cell functions and/or a B-cell activation defect.

**Defective TCR-induced proliferation and signaling in the absence of αPIX.** The reduced numbers of αPIX$^-$ lymphocytes and reduced immune responses of αPIX$^-$ mice suggested cellular defects in T and/or B cells. We next investigated the consequences of αPIX mutation for T cells. In cellular proliferation assays, αPIX$^-$ T-cell proliferation was measured in vitro using purified CD4$^+$ T cells that were stimulated for 3 days with anti-CD3 (TCR) alone, anti-CD3 (TCR) plus anti-CD28, ConA, or PMA plus ionomycin. Stimulation of CD3 alone or of CD3 plus CD28 revealed a consistent decrease in the proliferation of αPIX-deficient CD4$^+$ cells compared to wild-type cells (Fig. 4A). αPIX-deficient CD4$^+$ cells also showed substantially reduced proliferation in response to ConA. However, proliferation induced by PMA plus ionomycin, which bypasses TCR signaling, was normal, demonstrating that there were no intrinsic cell cycle defects in αPIX-deficient T cells (Fig. 4A). Next, αPIX$^-$ cells were tested for production of IL-2, also a readout for the activation of T cells. In agreement with the reduced TCR-induced proliferation, levels of IL-2 secreted by αPIX$^-$ T cells were also decreased following stimulation by anti-CD3 or ConA (Fig. 4B). Again, PMA plus ionomycin induced normal levels of IL-2, indicating that the production and secretion of IL-2 was not affected by loss of αPIX. Since these data pointed to defects in T-cell activation, the basal activation state of αPIX$^-$ T cells was assessed using flow cytometry of surface expression markers. There was no difference in the expression of the T-cell activation markers CD25 (IL-2 receptor α chain) or CD69 between knockout and wild-type mice (data not shown).

The defects in T-cell proliferation suggested a defect in signaling from the TCR. We therefore tested a range of TCR-stimulated outputs in αPIX$^-$ T cells. TCR stimulation of calcium flux (Fig. 5A) and actin polymerization (Fig. 5B) was normal in αPIX$^-$ T cells. TCR stimulation of overall tyrosine phosphorylation in αPIX$^-$ T cells was also normal (Fig. 5C). Since PIX proteins are RhoGEFs for Rac1 and CDC42, we measured GTPase activation using a GTP capture assay in TCR-stimulated T cells. Unexpectedly, activation of both Rac1 and CDC42 in αPIX$^-$ T cells was normal (Fig. 5D and data not shown), suggesting that either αPIX is not an important GEF for TCR signaling or that βPIX can compensate for αPIX in this function. We then tested the phosphorylation of specific signaling molecules downstream of TCR. αPIX-deficient T cells showed normal phosphorylation of ERK1/2 mitogen-activated protein kinases following anti-CD3 stimulation (Fig. 5E). Moreover, phosphorylation of the αPIX binding partner c-Cbl was also unchanged in PIX-deficient T cells (Fig. 5E). Thus, αPIX does not seem to be important to proximal TCR signaling. However, using a phospho antibody specific for serine residues in the PIX-binding site of both PAK1 and PAK2, we found that TCR-induced phosphorylation of PAK was markedly reduced in αPIX-deficient T cells compared to wild-type T cells (Fig. 5F). Together, these data show that αPIX is important in T cells in regulating TCR signaling to proliferation and to PAK activation.

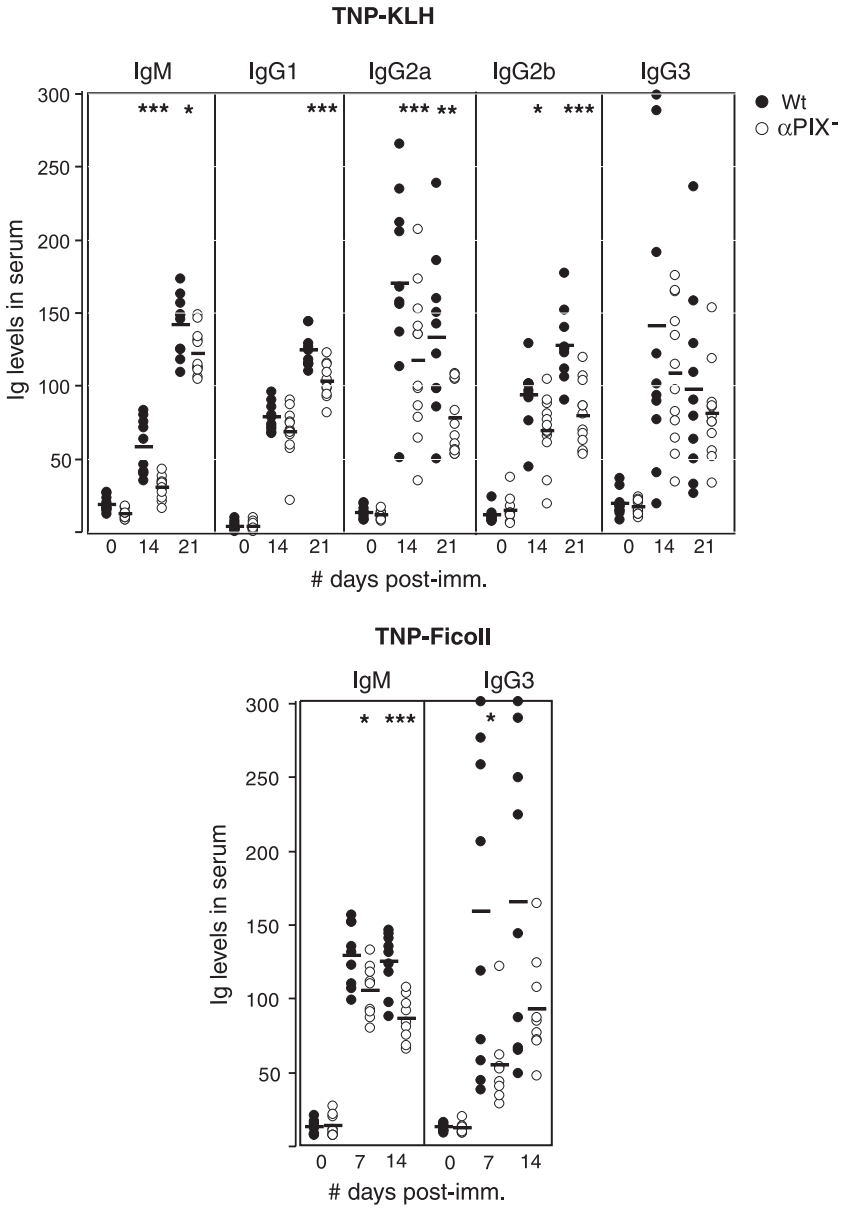


FIG. 3. Decreased humoral immune responses in αPIX$^-$ mice. Wild-type (Wt) and αPIX$^-$ mice (12 to 14 weeks old) were immunized with the thymus-dependent antigen TNP-KLH (10 Wt and 12 αPIX$^-$ mice) or the thymus-independent type 2 antigen TNP-Ficoll (10 Wt and 10 αPIX$^-$ mice). Primary TNP-KLH immune responses were measured after 14 days. Mice were challenged on day 14, and secondary immune responses were assessed on day 21. TNP-Ficoll immune responses were analyzed on day 7 and day 14. Significance was verified by Student's *t* test. *, $P < 0.05$; **, $P < 0.01$; ***, $P < 0.001$.

**αPIX is required for GIT2 expression.** PIX proteins are implicated in proteolysis through direct binding to two ubiquitin ligases and the common subunit of calpain proteases (18, 28, 48). In addition, βPIX stabilizes GIT2 expression in HeLa cells (19). To determine if GIT and other signaling proteins that interact with PIX proteins are expressed normally in αPIX$^-$ T cells, we performed Western blot analysis of PAK2, the main PAK isoform in murine T cells (14), c-Cbl, SAP, Rac1, Cdc42, GIT1, and GIT2. No differences were found in the expression of c-Cbl, SAP, Rac1, or CDC42. GIT expression was analyzed with an anti-GIT antibody that recognizes both GIT1 and GIT2. Although these proteins are of similar molecular masses (approximately 95 kDa), the higher-molecular-mass protein recognized by this antibody is GIT1, and the lower-molecular-mass protein is GIT2 (19). In T cells, we observed two bands of similar size and found that the band corresponding in size to GIT2 showed stronger expression than GIT1 (Fig. 6A). The identity of the protein corresponding to the size of GIT1 in T cells was confirmed using a second antibody against GIT1 (Fig. 6A). No differences between wild-type and αPIX$^-$ T cells in GIT1 expression were observed (Fig. 6A). In marked contrast, the GIT2 corresponding band was strongly reduced in αPIX$^-$ T cells (Fig. 6A). We also found a similar reduction of GIT2 in B cells (data not

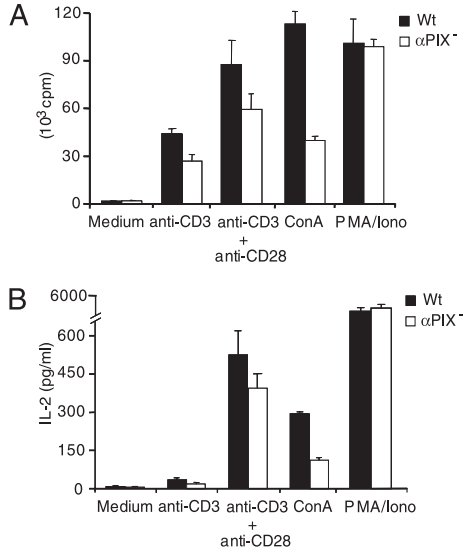


FIG. 4. TCR-induced cellular responses. (A) Decreased TCR-induced proliferation of αPIX$^-$ T cells. Proliferation of wild-type (Wt) or αPIX$^-$ CD4$^+$ T cells was assessed after stimulation with coated anti-CD3 alone or with anti-CD28, ConA, or PMA plus ionomycin and measured by [$^3$H]thymidine incorporation. (B) IL-2 production by αPIX$^-$ T cells. CD4$^+$ T cells were stimulated as indicated for panel A, and IL-2 collected 16 h later from cell supernatants was assessed by ELISA. Data are expressed as means ± standard deviations of triplicate values and are representative of four independent experiments.

shown). These data indicate that αPIX stabilizes GIT2 in lymphocytes.

To determine whether αPIX was a regulator of transcriptional or posttranscriptional expression of GIT2, we performed Northern blot analysis of mRNA from lymph node cells. Two forms of GIT2 mRNA, termed GIT2-long and GIT2-short, have been characterized in humans (35, 44), and equivalent bands of similar sizes were observed in wild-type and αPIX$^-$ T cells with normal amounts and intensities (Fig. 6B). mRNA results were confirmed using quantitative PCR and primers corresponding to the N termini of GIT2-long and GIT2-short and to the C terminus of GIT2-long. GIT2 mRNA levels were normal compared to the wild type (Fig. 6C). The normal expression of GIT2 mRNA suggested either translational or posttranslational defects in GIT2 protein. To investigate this, we used an antibody that recognizes both GIT2 isoforms to perform Western blotting with lymph node T-cell extracts. We found that GIT2-long was strongly reduced in αPIX$^-$ T cells and not seen on short exposures of film, as shown in Fig. 6D, but was faintly visible on longer exposures (data not shown). However, GIT2-short was still present, suggesting that GIT2-long is degraded in the absence of αPIX (Fig. 6D). To further investigate the possibility that GIT2-long was subjected to abnormal degradation in αPIX$^-$ T cells, we tested extracts from wild-type cells treated with cycloheximide to inhibit new protein synthesis. In untreated wild-type cells, both GIT2-long and

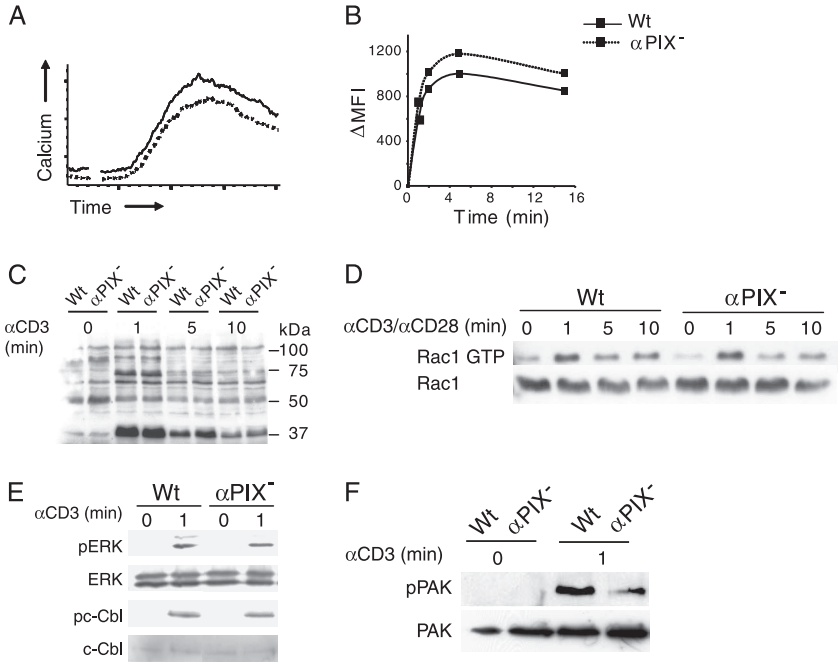


FIG. 5. αPIX in TCR signaling. (A) Normal calcium fluxing. Lymph node T cells from wild-type (Wt) and αPIX$^-$ mice were stained with calcium-sensitive dyes and, for Thy1, stimulated on TCR and analyzed by FACS. (B) Normal actin polymerization. Lymph node T cells were stimulated on TCR, fixed, stained with FITC-phalloidin and anti-CD4, and analyzed by FACS. (C) Normal tyrosine phosphorylation in αPIX$^-$ T cells. Purified lymph node T cells from wild-type (Wt) or αPIX$^-$ mice were stimulated on TCR (CD3) for the indicated times (minutes), and lysates were resolved by SDS-PAGE and immunoblotted for proteins phosphorylated on tyrosine residues. (D) Normal GTPase activation. Purified lymph node T cells from wild-type and αPIX$^-$ mice were stimulated on TCR. Cell extracts were incubated with glutathione *S*-transferase–PAK1 RBD to precipitate GTP-bound Rac1 (Rac1-GTP). Anti-Rac1 antibodies were used to detect GTP-bound GTPases. To confirm equal loading, 10% of cell lysates was resolved separately and immunoblotted using anti-Rac. (E) Normal ERK1/2 and c-Cbl phosphorylation. Purified lymph node T cells were stimulated on TCR and CD28 and analyzed for ERK1/2, Cbl, and PAK phosphorylation using phospho-specific antibodies. (F) Defective PAK phosphorylation in αPIX-deficient T cells. Purified lymph node T cells were stimulated on TCR and CD28 and analyzed for PAK phosphorylation using phospho-specific antibodies. Antibodies against the nonphosphorylated proteins served as a control. All data are representative of at least three independent experiments.

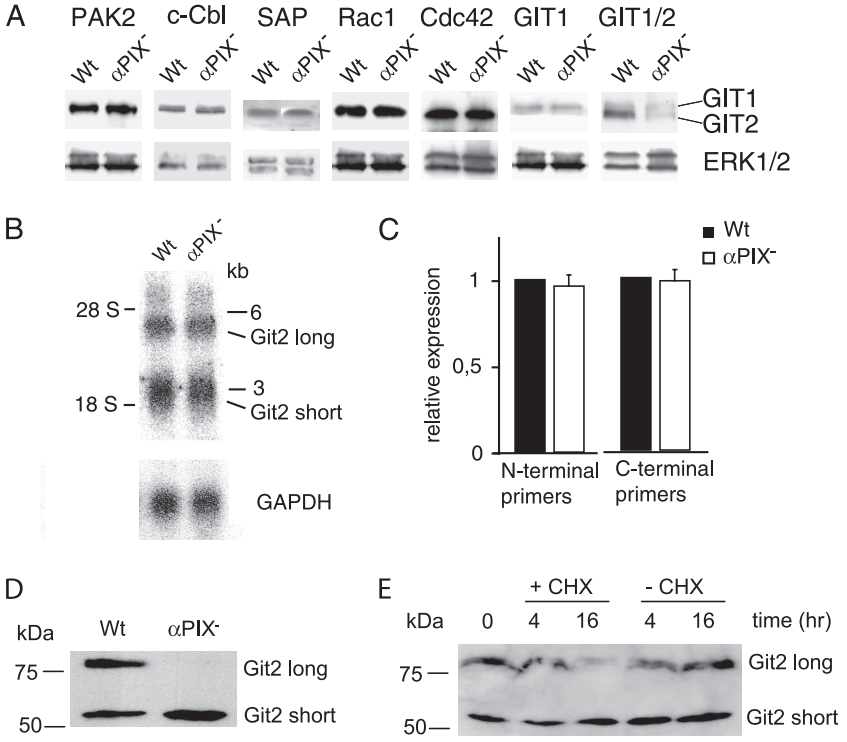


FIG. 6. αPIX is required for GIT2 expression. (A) Decreased GIT2 protein levels. Purified lymph node T cells were analyzed for the expression of PIX-associated proteins PAK2, Cbl, SAP, Rac1, CDC42, GIT1, and GIT1/2 by Western blotting. The identities of the bands corresponding to GIT1 and GIT2 in the lane probed with anti-GIT1/2 are indicated. The blot was reprobed with anti-ERK1/2 to demonstrate equal loading. (B) Normal GIT2 mRNA expression. GIT2 expression in splenocytes was analyzed by Northern blotting using an N-terminal probe recognizing GIT2-long and GIT2-short. The positions of RNA molecular markers are indicated. (C) Quantitative PCR. Expression analysis of GIT2 in purified T cells by real-time PCR using primers recognizing either GIT2-long and GIT2-short (N-terminal primers) or primers specific for GIT2-long (C-terminal primers). (D) GIT2-short protein expression. Expression of GIT2 proteins was determined in T cells using an antibody recognizing GIT2-long and GIT2-short only and not GIT1. (E) In vitro GIT2 turnover in T cells. Purified wild-type T cells were cultured on plates coated with anti-CD3 (5 μg) and soluble anti-CD28 antibody (1 μg) with or without 50 μg/ml of cycloheximide (CHX) for the indicated times and analyzed for GIT2 expression by Western blotting.

GIT2-short are observed throughout a time course. However, in treated cells GIT2-long gradually disappears, indicating that it is subject to turnover in about 16 h. In contrast, GIT2-short is detectable at all time points and is thus not degraded and replaced (Fig. 6E). These results indicate that the pool of GIT2-long protein is normally replenished in wild-type T cells but not in αPIX$^-$ T cells. Together, these data show that αPIX stabilizes GIT2-long protein in lymphocytes.

**Defective migration of αPIX$^-$ lymphocytes.** PIX proteins have been implicated in cytoskeletal functions, such as cell spreading and focal complexes (48, 50). GIT2 is an inhibitor of epithelial cell migration (19). Therefore, we tested spontaneous migration of αPIX$^-$ T and B cells and chemokine-induced migration to SDF-1α (CXCL12) using flow cytometry analysis of the output of a transwell chamber. We found that the number of αPIX$^-$ T cells migrating to SDF-1α was consistently higher than that of the wild type (Fig. 7A). However, the migration of the uninduced sample was also increased, suggesting that the basal migration rate of αPIX$^-$ T cells was higher than the wild type (Fig. 7A). Additional testing of αPIX$^-$ T-cell migration in the absence of stimuli confirmed that the αPIX$^-$ basal migration was higher than in the wild type (Fig. 7B). Similar results were observed in αPIX$^-$ B cells (Fig. 7A and B, lower panels). Lymphocytes squeezing through a restrictive extracellular matrix radically deform their shape in an amoeboid movement (20). To discover if αPIX regulates this type of migration, we tested migration through membranes of smaller pore sizes, 3 μm instead of 5 μm, as was previously described for βPIX (57). Overall migration rates were reduced 5- to 10-fold, but we found similar results as in Fig. 7A and B: αPIX$^-$ cells migrated consistently more than wild-type cells (data not shown). Together, these data show that αPIX is an inhibitor of lymphocyte migration.

**αPIX is required for immune synapses.** The contact zone between a T cell and an antigen-presenting cell (APC) consists of an organized arrangement of adhesion and signaling molecules known as the immune synapse (13). It has been shown that PIX proteins and PAK are recruited to the interface between T cells and APCs (43). To test PAK2 recruitment to the αPIX-deficient immune synapse, αPIX$^-$ mice were first crossed to OT-II TCR-Tg mice that have a TCR specific for the ovalbumin epitope from amino acids 323 through 339 ($OVA_{323–339}$) presented by I-Ab MHC class II (5). OVA peptide-loaded B cells were used as APCs and were mixed with T cells to initiate conjugates and immune synapse formation. As shown in Fig. 8, TCR localization to the synapse was not affected by the loss of αPIX. The antibody used to detect PIX recognizes both αPIX and βPIX (34), therefore both isoforms

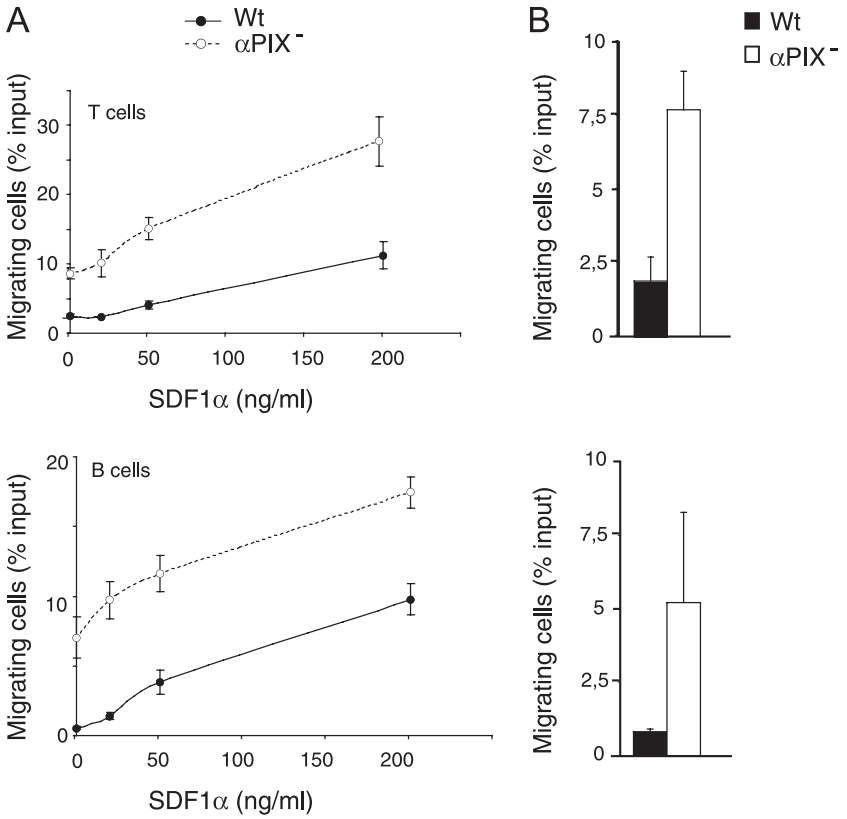


FIG. 7. Elevated T- and B-cell migration. $CD4^+$ T cells (upper panels) and $B220^+$ B cells (lower panels) from wild-type (Wt) or $\alpha PIX^-$ mice were tested for chemokine-induced (A) or spontaneous (B) migration through the filter of a transwell plate (5 μm). Results are shown as the percentage of input cells that migrated to the lower chamber containing either increasing concentrations of SDF-1α (CXCL12) (A) or medium alone (B). Data are expressed as the means ± standard deviations and represent at least three independent experiments.

should be present in wild-type cells while only βPIX should be found in $\alpha PIX^-$ T cells. Indeed, βPIX was recruited to the synapse in $\alpha PIX^-$ T cells (Fig. 8). Confirming a role for αPIX in PAK activation, TCR-stimulated recruitment of PAK2 to the synapse was substantially reduced in $\alpha PIX^-$ T cells. Moreover, there was a corresponding decrease in PAK2 phosphorylation at the synapse (Fig. 8). These data show that αPIX is required for strong and efficient phosphorylation of PAK at the synapse and that βPIX cannot compensate for αPIX in this function.

We next used flow cytometry to quantify the ability of $\alpha PIX^-$ T cells to form synapses by counting conjugates formed, as in Fig. 8. We observed approximately twofold more B-cell conjugates with wild-type T cells than with $\alpha PIX^-$ T cells, after subtracting the number of T-cell–APC conjugates that were not specifically induced by TCR bound to peptide (Fig. 9A). Expression of OT-II TCR (measured by surface Vα2 expression) and integrins important for T cells (LFA-1 [αLβ2] and VLA-4 [α4β1]) was similar between wild-type and $\alpha PIX^-$ T cells, therefore the defect in conjugate formation was not due to lack of these adhesion molecules (Fig. 9B and data not shown).

The antigen-activated TCR signals to integrins such as Lfa-1 in a process referred to as inside-out signaling and drives accumulation of Lfa-1 at the synapse (46). The defects in $\alpha PIX^-$ conjugate formation prompted us to test whether Lfa-1 was properly recruited to the immune synapse of $\alpha PIX^-$ T cells. Lfa-1 clustering in $\alpha PIX^-$ T-cell conjugates was assessed by staining for the CD11a (αL) subunit of Lfa-1. Conjugates with wild-type T cells showed distinct and clear polarization of Lfa-1 at the synapse (Fig. 9C). In contrast, staining for Lfa-1 in $\alpha PIX^-$ T-cell synapses was weaker, and fewer conjugates with clustered Lfa-1 were observed (Fig. 9C). We counted conjugates featuring strong, polarized fluorescence for Lfa-1 at the synapse and found about twofold more in wild-type than in $\alpha PIX^-$ conjugates (Fig. 9C). Taken together, these data suggest that αPIX regulates immune synapse formation by linking TCR activation to PAK recruitment and Lfa-1 clustering.

**Defective B-cell proliferation in the absence of αPIX.** Since B-cell numbers were also reduced in $\alpha PIX^-$ mice, we next investigated cellular functions of $\alpha PIX^-$ B cells. In proliferation assays, $\alpha PIX^-$ B cells showed a severe reduction in proliferation after stimulation by either B7.6 or $F(ab')_2$ anti-IgM antibodies against the BCR (approximately 70% and 80% inhibition, respectively). However, proliferation induced by LPS was normal, demonstrating that there were no intrinsic cell cycle defects in αPIX-deficient B cells and that αPIX is not downstream of LPS receptors (Fig. 10A). These defects were lessened when costimulation with anti-CD40 or IL-4 was introduced (Fig. 10A), suggesting that additional stimuli can compensate for the BCR defect in $\alpha PIX^-$ B cells. To further explore the activation defects of $\alpha PIX^-$ B cells, we quantified

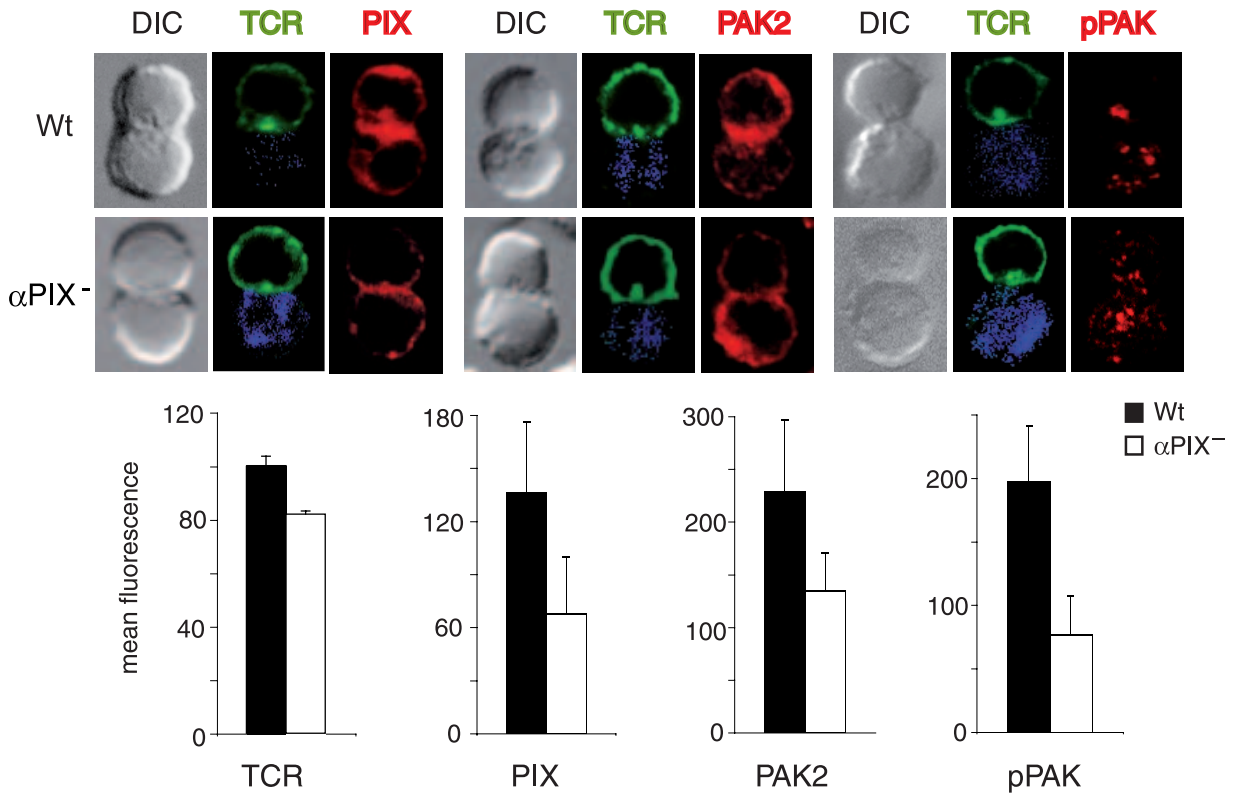


FIG. 8. Reduced recruitment of PAK to the T-cell–APC contact site in αPIX⁻ T cells. T-cell–B-cell conjugates were formed by mixing LPS-activated B cells pulsed with Ova II peptide and stained with CMAC (blue) with OT-II-transgenic CD4⁺ lymph node T cells from wild-type and αPIX⁻ mice. T cells were stained with anti-CD3–FITC (TCR; green). Cell conjugates are shown in differential interference contrast images. PIX, PAK2, and pPAK were stained with anti-PIX, anti-PAK2, and anti-pPAK antibodies and an Alexa 594 (red) secondary antibody (upper panels). The histogram represents the mean fluorescent intensity of TCR, PIX, PAK, or pPAK at the immune synapse (± the standard deviation), defined here as the interface between a T cell and a B cell featuring concentrated TCR fluorescence. Fluorescent intensity was assessed within a region that was redrawn for each protein at each synapse, with the background subtracted. Over 50 T-cell–B-cell conjugates were analyzed in each of two independent experiments.

cell surface levels of B-cell activation markers. Levels of MHC class II were about 1.5- to 2-fold lower on resting αPIX⁻ B cells. After 9 h of BCR stimulation, MHC class II levels were increased on αPIX⁻ B cells but did not rise to normal levels (Fig. 10B). Expression of CD69 on αPIX⁻ B cells was also decreased relative to the wild type after 6 h of anti-IgM stimulation but rose to normal levels after 16 h of activation (data not shown), indicating that αPIX is required for early BCR signaling to activation.

**αPIX is required for BCR signaling to PAK.** The BCR-induced proliferation defects pointed to potential problems in BCR signaling in αPIX⁻ B cells. Therefore, we next analyzed BCR proximal signaling in αPIX⁻ B cells and found some differences between αPIX⁻ T cells and B cells. Calcium fluxing in response to BCR stimulation was normal in αPIX⁻ B cells, as for αPIX⁻ T cells (Fig. 11B). BCR-directed tyrosine phosphorylation and ERK activation were slightly increased in αPIX⁻ B cells, in contrast to the normal results with αPIX⁻ T cells (Fig. 11A and C). However, similar to αPIX⁻ T cells, BCR-induced phosphorylation of PAK was also reduced in αPIX-deficient B cells compared to wild-type cells (Fig. 11D). We also found that GIT2-long protein expression was greatly reduced in αPIX⁻ B cells, similar to αPIX⁻ T cells (data not shown). Together, these results establish a role for αPIX downstream of the B-cell receptor and reveal some differences in αPIX roles between T cells and B cells.

## DISCUSSION

We report here about lymphocytes from mice deficient in αPIX, a member of the RhoGEF family of signaling and activating proteins. We first investigated the expression of αPIX and showed that it was specifically expressed in immune cells. In αPIX⁻ mice, mature lymphocyte populations were reduced in number and immune responses were weakened. At a cellular level, both αPIX⁻ T and B cells proliferated poorly to antigen receptor stimulation but migrated faster than the wild type. At a molecular level, GIT2-long protein was largely absent and PAK had reduced phosphorylation in response to TCR stimulation in αPIX⁻ lymphocytes. αPIX⁻ T cells were also defective in immune synapse formation: PAK and the Lfa-1 integrin subunit αL were not efficiently recruited to the synapse. Thus, our data suggest that αPIX regulates Lfa-1 integrin functions via a protein complex containing GIT2 and PAK. The lack of a relatively more severe immune phenotype is likely due to compensation by βPIX.

βPIX is a close homolog of αPIX. We wanted to determine the phenotypes of mice lacking either αPIX or βPIX alone

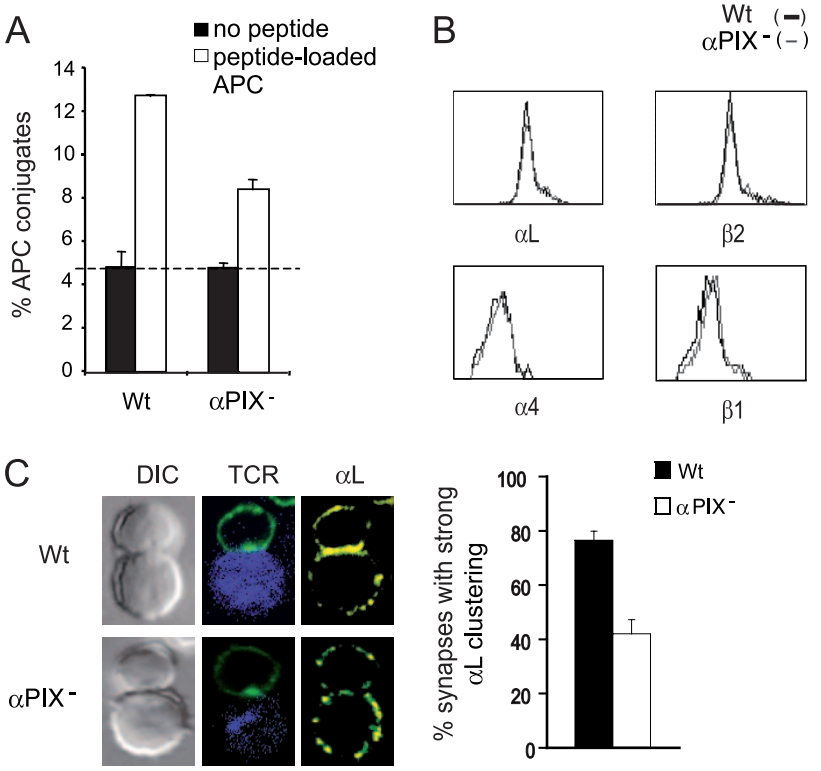


FIG. 9. Defective immune synapse formation in αPIX$^-$ T cells. (A) Reduced numbers of αPIX$^-$ T-cell–B-cell conjugates. Purified OT-II CD4$^+$ lymph node T cells from wild-type or αPIX$^-$ transgenic mice and B cells either loaded with OVA II peptide or left without peptide were stained with CFSE (T cells) and CMTMR (B cells). Equal numbers of CD4$^+$ T cells and APCs were mixed and analyzed for conjugate formation by FACS. APCs were gated and analyzed for the presence of CD4$^+$ cells. The dashed line divides numbers of conjugates that were specifically induced by peptide from background numbers of uninduced conjugates. Results are representative of three independent experiments performed in duplicate. (B) Normal integrin expression. CD4$^+$ cells from OT-II TCR transgenic wild-type or αPIX$^-$ mice were stained for α4, αL, β1, and β2 integrin chains and analyzed by FACS. (C) Reduced αL recruitment. T-cell–B-cell conjugates formed with OT-II CD4$^+$ T cells and peptide-loaded APCs (blue) were stained with anti-CD3–FITC (TCR; green) and anti-CD11a–biotin (αL; a component of Lfa-1 integrin), followed by streptavidin-Cy3 (light green). The histogram (right) shows the percentage of 200 T-cell–B-cell conjugates of wild-type and αPIX$^-$ synapses with polarized αL. Data are representative of three independent experiments.

before analyzing mice with combined mutations in both PIX proteins. In ongoing work, we found that mutation of βPIX alone is embryonic lethal at an early stage (data not shown). Unlike αPIX, βPIX is widely expressed, albeit also highly in immune cells. The broad expression of βPIX is consistent with the lethal phenotype, while the restricted expression of αPIX is in line with the more moderate phenotype we describe here. Additionally, the expression pattern of PIX proteins suggests that αPIX has evolved for some specific immune function. For example, the fact that αPIX has a CH domain while βPIX does not may influence the composition of protein complexes that form around αPIX, determining the specific immune function of αPIX. CH domains are often found in proteins that have a strong relationship to the cytoskeleton and may modify actin filaments (51).

We found that αPIX was required to stabilize GIT2-long protein, consistent with a previous report showing that βPIX regulates GIT2 protein levels in HeLa cells (19). A similar function has been reported for adhesion and degranulation promoting adaptor protein (ADAP) and its binding partner, SKAP55 (27). ADAP and SKAP55 relay TCR signals to integrin adhesion (37). In the absence of ADAP, SKAP55 and its close homolog, SKAP-HOM, are constitutively degraded (27). Thus, T cells from ADAP knockout mice are actually triple knockouts for ADAP, SKAP55, and SKAP-HOM. Similarly, the αPIX$^-$ lymphocytes are akin to a double knockout of αPIX and GIT2-long. PIX and GIT proteins associate tightly in a large, stable oligomeric complex that could contain as many as 10 to 20 proteins of the approximate size of PIX and GIT proteins (45). PIX and GIT proteins do not disassociate from each other freely nor can they be assembled into the complex in a preparation of purified proteins, and it was suggested that this is because in vivo they are cotranslationally assembled into a complex (45). Therefore, αPIX may stabilize GIT2-long by binding tightly to it in the PIX-GIT complex and preventing it from being accessible to protease cleavage or ubiquitin tagging. Since αPIX also binds to a common calpain protease subunit and to two ubiquitin ligases (18, 28, 48), it may act as a protective barrier between these and GIT2-long. This would be important in cellular microenvironments regulated by high protein turnover, such as focal complexes at the membrane.

We have shown that αPIX knockout lymphocytes lack GIT2-long protein; however, GIT2-short was still expressed. GIT2-short lacks the paxillin-binding site and the coiled-coil domain involved in dimerization of GIT1 and GIT2-long and is differently localized at the perinuclear regions (35). It has been

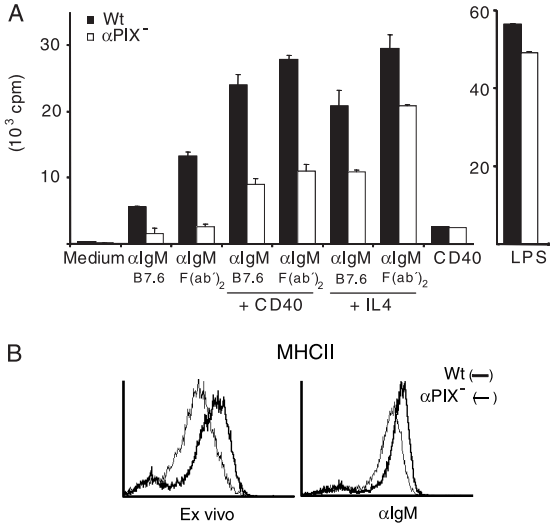


FIG. 10. Reduced BCR-induced proliferation and MHC-II expression in αPIX⁻ mice. (A) Purified wild-type and αPIX⁻ splenic B cells were stimulated with medium alone or with anti-IgM MAb B7.6 or anti-IgM F(ab′)$_2$ plus, where indicated, anti-CD40 or IL-4, or with LPS, and proliferation was measured by [$^3$H]thymidine incorporation. Data are means ± standard deviations of triplicate values and are representative of four experiments. (B) Reduced MHC-II expression on αPIX-deficient B cells. Purified splenic B220$^+$ cells from wild-type and αPIX mutant mice were stained for MHC-II directly after purification or after a 9-hour stimulation with anti-IgM. Similar results were obtained in two different experiments.

suggested that GIT2-short regulates Golgi complex organization rather than focal complexes (35). Little is known about GIT2 in lymphocytes, as the knockout phenotype, like that of αPIX, has only been characterized in neutrophils (36). It will be important for the understanding of the PIX-GIT complex to establish which defects in the αPIX lymphocytes are due to loss of αPIX and which are due to loss of GIT2-long.

Although PIX is a RhoGEF, we did not observe any defects in TCR activation of PIX targets Rac1 and Cdc42 in αPIX⁻ T cells. This result was surprising, since it was reported that in αPIX⁻ neutrophils Cdc42 activation by C5a is impaired, and we expected a similar result for lymphocytes (33). One possible explanation for the difference is that the GTPases in the neutrophil study were activated by C5a, a G-protein-coupled receptor which may differ in signaling requirements than the TCR that we assessed. Alternatively, it may be the case that αPIX⁻ neutrophils have a severe signaling defect in the PIX-GIT complex, since neutrophils do not express GIT1 (36). Thus, αPIX⁻ neutrophils lack αPIX, GIT1, and likely GIT2-long, which could impair signaling to GTPases more than in αPIX⁻ lymphocytes, as they still express GIT1. Another possible explanation for the normal GTPase activation in αPIX⁻ lymphocytes may be that βPIX can compensate for αPIX in GTPase activation. There is evidence from studies on Jurkat cells that mice with double mutations in αPIX and βPIX could potentially have defective GTPase activation. It was shown that Jurkat T cells overexpressing a mutant SH3 domain from βPIX have defective calcium fluxing and phospholipase C-γ1 activation (43). The mutant SH3 domain from βPIX probably outcompetes endogenous αPIX and βPIX in binding to signaling components, effectively creating cells with a double inactivation of αPIX and βPIX that manifest stronger signaling defects than those of the αPIX knockout T cells described here. Thus, the normal calcium fluxing, actin polymerization, and GTPase activation we observed may be due to compensation by βPIX.

Another observation that emerged from this study is that αPIX⁻ lymphocytes migrated more than wild-type cells, indicating that αPIX is an inhibitor of lymphocyte migration. A previous report showed that GIT2 also represses cell motility by inhibiting lamellipodia (19). PIX and GIT proteins bind to many proteins involved in focal complexes, such as paxillin, a scaffold-type protein that is central to focal adhesions (25, 50). It is therefore a strong possibility that αPIX and GIT2 inhibit

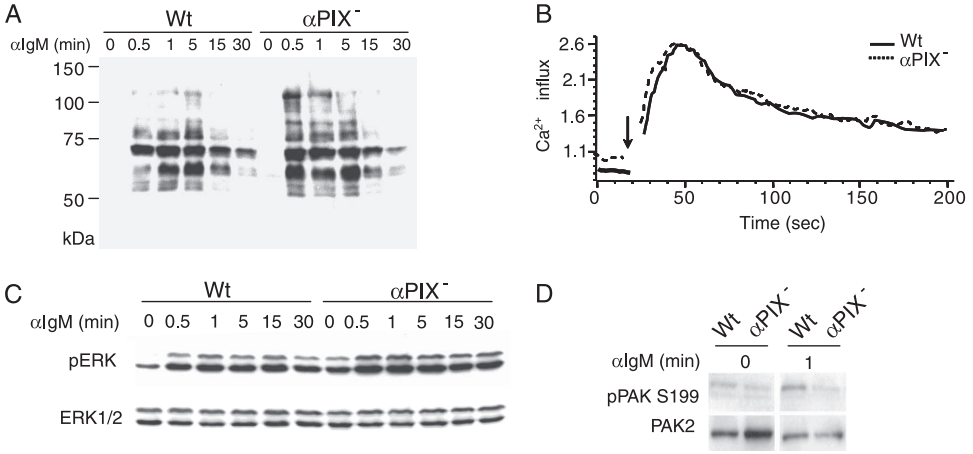


FIG. 11. Altered BCR signaling in αPIX⁻ B cells. (A) Increased tyrosine phosphorylation. Lysates from purified wild-type (Wt) or αPIX⁻ splenic B cells stimulated with F(ab′)$_2$ anti-IgM (10 μg/ml) for the indicated times were analyzed for phosphotyrosine. (B) Normal BCR-induced calcium flux. B cells from wild-type and αPIX⁻ mice were stained with calcium-sensitive dyes and for B220 surface expression, stimulated on BCR by F(ab′)$_2$ anti-IgM, and analyzed by FACS. (C) Increased ERK activation. Cell lysates prepared as for panel A were immunoblotted for phospho-ERK. Blots were stripped and reprobed for ERK1/2 as loading controls. (D) Defective PAK phosphorylation in αPIX⁻ B cells. Purified splenic B cells were stimulated on BCR by F(ab′)$_2$ anti-IgM and analyzed for PAK phosphorylation using phospho-specific antibodies. Blots were stripped and reprobed for PAK2 as a loading control.

cell migration by participating in focal complexes such as those required during interaction between a T cell and an antigen-presenting cell. A defect in focal adhesions could explain both the increased migration of αPIX$^-$ T cells and the defective immune synapses of αPIX$^-$ T cells. We found that PAK was not efficiently recruited to or activated at immune synapses on αPIX$^-$ T cells, consistent with a previous report showing impaired recruitment and activation of PAK in Jurkat cells (43). We also found that Lfa-1 clusters at αPIX$^-$ immune synapses were reduced, as were overall numbers of αPIX$^-$ immune synapses. Since Lfa-1 is an integrin that regulates adhesion of T cells to APCs, our results are consistent with a model of αPIX as a regulator of adhesion complexes formed upon TCR activation that restrain a T cell from migrating and allow it to form a contact zone with another cell.

Activation of TCR results in inside-out signaling to integrins, including Lfa-1 (11, 29). Some of the known signaling proteins in this pathway include ADAP and SKAP55. SKAP-HOM regulates BCR activation of adhesion in B cells (56). Many parallels between the phenotypes of these mice with that of αPIX$^-$ mice suggest that αPIX may function in the same pathway. First, Lfa-1 and ADAP knockout mice both have decreased lymphocyte cellularity in the periphery, presumably due to a role for Lfa-1 in adhesion during lymphocyte recirculation (8, 22, 42, 52). Similarly, αPIX$^-$ lymphocytes migrated excessively and may migrate out of their developmental niches in the spleen and lymph nodes due a failure to adhere to the extracellular matrix, resulting in decreased cell numbers. In addition, Lfa-1 and ADAP are both required for normal T-cell proliferation (8, 22, 42, 52), consistent with our finding that αPIX is required for both T- and B-cell proliferation. Moreover, ADAP, SKAP55, and Lfa-1 are all implicated in T-cell–APC conjugation or synapse formation (38, 58, 59). We also found that efficiency of conjugation and the recruitment of Lfa-1 and PAK to the synapse were all decreased in the absence of αPIX. Finally, proximal TCR signaling events in ADAP knockout T cells, such as tyrosine phosphorylation, calcium fluxing, actin polymerization, and ERK activation, were normal (22, 42); proximal BCR signaling events in SKAP-HOM B cells, such as tyrosine phosphorylation, calcium fluxing, and ERK activation, were also normal (56). We found that these events were normal in αPIX$^-$ T cells, too, and virtually normal in αPIX$^-$ B cells. The similarities in these phenotypes suggest that like ADAP and SKAP proteins, αPIX plays a role in TCR activation of focal complexes that is independent of immediate TCR signaling events. Further studies are required to investigate these propositions, and these experiments are under way in our laboratory.

In conclusion, we have identified an essential role for αPIX in both T cells and B cells in lymphocyte development and immune functions. The disruption of αPIX resulted in wide-ranging defects in lymphocytes. It has been shown that in neuronal cells, PIX proteins regulate critical functions: βPIX binds to neuronal proteins and regulates neurite extension (53, 61), and αPIX mutation is linked to mental retardation (32). Our results now highlight the importance of the PIX-GIT complex to lymphocytes and suggest that investigating the parallels between neurons and lymphocytes will provide insights that may contribute to understanding pathological disorders in both systems. Future issues to be resolved are the role of the PIX-GIT complex in membrane dynamics at lymphocyte adhesions: perhaps PIX proteins control actin extensions such as lamellipodia or filopodia, while GIT proteins transport membrane vesicles to the site of cellular extension. It also will be interesting to assess the roles of αPIX in other immune cell types, such as macrophages or dendritic cells. For example, mutation of αPIX may also affect the functioning of the B-cell synapse (7). Finally, it is conceivable that the phenotype of mice with an αPIX mutation combined with a conditional βPIX mutation will be more severe than that of αPIX$^-$ mice, and the analysis of the double knockout mice will reveal mechanistic insights into synapse formation and lymphocyte migration.

## ACKNOWLEDGMENTS

We thank N. Ushmorova for excellent technical assistance, I. Girkontaite for scientific support, and K. Tedford for scientific editing. We also thank Ed Manser for the gift of αPIX polyclonal antibody.

This work was supported by Deutsche Forschungsgemeinschaft grants SFB 497 and DFG Fi-639/2-2 to K.D.F. K.M. is supported by a Marie Curie Fellowship (contract HPMF-CT-1999-00128).

## REFERENCES

1. **Audebert, S., C. Navarro, C. Nourry, S. Chasserot-Golaz, P. Lecine, Y. Bellaiche, J. L. Dupont, R. T. Premont, C. Sempere, J. M. Strub, A. Van Dorsselaer, N. Vitale, and J. P. Borg.** 2004. Mammalian Scribble forms a tight complex with the βPIX exchange factor. Curr. Biol. **14:**987–995.
2. **Bagrodia, S., S. J. Taylor, K. A. Jordon, L. Van Aelst, and R. A. Cerione.** 1998. A novel regulator of p21-activated kinases. J. Biol. Chem. **273:**23633–23636.
3. **Baird, D., Q. Feng, and R. A. Cerione.** 2005. The Cool-2/α-Pix protein mediates a Cdc42-Rac signaling cascade. Curr. Biol. **15:**1–10.
4. **Balazs, M., F. Martin, T. Zhou, and J. Kearney.** 2002. Blood dendritic cells interact with splenic marginal zone B cells to initiate T-independent immune responses. Immunity **17:**341–352.
5. **Barnden, M. J., J. Allison, W. R. Heath, and F. R. Carbone.** 1998. Defective TCR expression in transgenic mice constructed using cDNA-based alpha- and beta-chain genes under the control of heterologous regulatory elements. Immunol. Cell Biol. **76:**34–40.
6. **Barreiro, O., H. de la Fuente, M. Mittelbrunn, and F. Sanchez-Madrid.** 2007. Functional insights on the polarized redistribution of leukocyte integrins and their ligands during leukocyte migration and immune interactions. Immunol. Rev. **218:**147–164.
7. **Batista, F. D., D. Iber, and M. S. Neuberger.** 2001. B cells acquire antigen from target cells after synapse formation. Nature **411:**489–494.
8. **Berlin-Rufenach, C., F. Otto, M. Mathies, J. Westermann, M. J. Owen, A. Hamann, and N. Hogg.** 1999. Lymphocyte migration in lymphocyte function-associated antigen (LFA)-1-deficient mice. J. Exp. Med. **189:**1467–1478.
9. **Brown, A., X. Wang, E. Sawai, and C. Cheng-Mayer.** 1999. Activation of the PAK-related kinase by human immunodeficiency virus type 1 Nef in primary human peripheral blood lymphocytes and macrophages leads to phosphorylation of a PIX-p95 complex. J. Virol. **73:**9899–9907.
10. **Brunner, C., A. Sindrilaru, I. Girkontaite, K. D. Fischer, C. Sunderkotter, and T. Wirth.** 2007. BOB.1/OBF.1 controls the balance of TH1 and TH2 immune responses. EMBO J. **26:**3191–3202.
11. **Burbach, B. J., R. B. Medeiros, K. L. Mueller, and Y. Shimizu.** 2007. T-cell receptor signaling to integrins. Immunol. Rev. **218:**65–81.
12. **Campa, F., N. Machuy, A. Klein, and T. Rudel.** 2006. A new interaction between Abi-1 and βPIX involved in PDGF-activated actin cytoskeleton reorganisation. Cell. Res. **16:**759–770.
13. **Cemerski, S., and A. Shaw.** 2006. Immune synapses in T-cell activation. Curr. Opin. Immunol. **18:**298–304.
14. **Chu, P. C., J. Wu, X. C. Liao, J. Pardo, H. Zhao, C. Li, M. K. Mendenhall, E. Pali, M. Shen, S. Yu, V. C. Taylor, G. Aversa, S. Molineaux, D. G. Payan, and E. S. Masuda.** 2004. A novel role for p21-activated protein kinase 2 in T cell activation. J. Immunol. **172:**7324–7334.
15. **Feng, Q., J. G. Albeck, R. A. Cerione, and W. Yang.** 2002. Regulation of the Cool/Pix proteins: key binding partners of the Cdc42/Rac targets, the p21-activated kinases. J. Biol. Chem. **277:**5644–5650.
16. **Feng, Q., D. Baird, and R. A. Cerione.** 2004. Novel regulatory mechanisms for the Dbl family guanine nucleotide exchange factor Cool-2/α-Pix. EMBO J. **23:**3492–3504.
17. **Fischer, K. D., Y. Y. Kong, H. Nishina, K. Tedford, L. E. Marengere, I. Kozieradzki, T. Sasaki, M. Starr, G. Chan, S. Gardener, M. P. Nghiem, D. Bouchard, M. Barbacid, A. Bernstein, and J. M. Penninger.** 1998. Vav is a

regulator of cytoskeletal reorganization mediated by the T-cell receptor. Curr. Biol. **8:**554–562.
18. **Flanders, J. A., Q. Feng, S. Bagrodia, M. T. Laux, A. Singavarapu, and R. A. Cerione.** 2003. The Cbl proteins are binding partners for the Cool/Pix family of p21-activated kinase-binding proteins. FEBS Lett. **550:**119–123.
19. **Frank, S. R., M. R. Adelstein, and S. H. Hansen.** 2006. GIT2 represses Crk- and Rac1-regulated cell spreading and Cdc42-mediated focal adhesion turnover. EMBO J. **25:**1848–1859.
20. **Friedl, P.** 2004. Prespecification and plasticity: shifting mechanisms of cell migration. Curr. Opin. Cell Biol. **16:**14–23.
21. **Girkontaite, I., K. Missy, V. Sakk, A. Harenberg, K. Tedford, T. Potzel, K. Pfeffer, and K. D. Fischer.** 2001. Lsc is required for marginal zone B cells, regulation of lymphocyte motility and immune responses. Nat. Immunol. **2:**855–862.
22. **Griffiths, E. K., C. Krawczyk, Y. Y. Kong, M. Raab, S. J. Hyduk, D. Bouchard, V. S. Chan, I. Kozieradzki, A. J. Oliveira-Dos-Santos, A. Wakeham, P. S. Ohashi, M. I. Cybulsky, C. E. Rudd, and J. M. Penninger.** 2001. Positive regulation of T cell activation and integrin adhesion by the adapter Fyb/Slap. Science **293:**2260–2263.
23. **Gu, C., S. G. Tangye, X. Sun, Y. Luo, Z. Lin, and J. Wu.** 2006. The X-linked lymphoproliferative disease gene product SAP associates with PAK-interacting exchange factor and participates in T cell activation. Proc. Natl. Acad. Sci. USA **103:**14447–14452.
24. **Harenberg, A., I. Girkontaite, K. Giehl, and K. D. Fischer.** 2005. The Lsc RhoGEF mediates signaling from thromboxane A2 to actin polymerization and apoptosis in thymocytes. Eur. J. Immunol. **35:**1977–1986.
25. **Hoefen, R. J., and B. C. Berk.** 2006. The multifunctional GIT family of proteins. J. Cell Sci. **119:**1469–1475.
26. **Hoffman, G. R., and R. A. Cerione.** 2002. Signaling to the Rho GTPases: networking with the DH domain. FEBS Lett. **513:**85–91.
27. **Huang, Y., D. D. Norton, P. Precht, J. L. Martindale, J. K. Burkhardt, and R. L. Wange.** 2005. Deficiency of ADAP/Fyb/SLAP-130 destabilizes SKAP55 in Jurkat T cells. J. Biol. Chem. **280:**23576–23583.
28. **Janz, J. M., T. P. Sakmar, and K. C. Min.** 2007. A novel interaction between atrophin-interacting protein 4 and beta-p21-activated kinase-interactive exchange factor is mediated by an SH3 domain. J. Biol. Chem. **282:**28893–28903.
29. **Kinashi, T.** 2005. Intracellular signalling controlling integrin activation in lymphocytes. Nat. Rev. Immunol. **5:**546–559.
30. **Koh, C. G., E. Manser, Z. S. Zhao, C. P. Ng, and L. Lim.** 2001. β1PIX, the PAK-interacting exchange factor, requires localization via a coiled-coil region to promote microvillus-like structures and membrane ruffles. J. Cell Sci. **114:**4239–4251.
31. **Ku, G. M., D. Yablonski, E. Manser, L. Lim, and A. Weiss.** 2001. A PAK1-PIX-PKL complex is activated by the T-cell receptor independent of Nck, Slp-76 and LAT. EMBO J. **20:**457–465.
32. **Kutsche, K., H. Yntema, A. Brandt, I. Jantke, H. G. Nothwang, U. Orth, M. G. Boavida, D. David, J. Chelly, J. P. Fryns, C. Moraine, H. H. Ropers, B. C. Hamel, H. van Bokhoven, and A. Gal.** 2000. Mutations in ARHGEF6, encoding a guanine nucleotide exchange factor for Rho GTPases, in patients with X-linked mental retardation. Nat. Genet. **26:**247–250.
33. **Li, Z., M. Hannigan, Z. Mo, B. Liu, W. Lu, Y. Wu, A. V. Smrcka, G. Wu, L. Li, M. Liu, C. K. Huang, and D. Wu.** 2003. Directional sensing requires G beta gamma-mediated PAK1 and PIX alpha-dependent activation of Cdc42. Cell **114:**215–227.
34. **Manser, E., T. H. Loo, C. G. Koh, Z. S. Zhao, X. Q. Chen, L. Tan, I. Tan, T. Leung, and L. Lim.** 1998. PAK kinases are directly coupled to the PIX family of nucleotide exchange factors. Mol. Cell **1:**183–192.
35. **Mazaki, Y., S. Hashimoto, K. Okawa, A. Tsubouchi, K. Nakamura, R. Yagi, H. Yano, A. Kondo, A. Iwamatsu, A. Mizoguchi, and H. Sabe.** 2001. An ADP-ribosylation factor GTPase-activating protein Git2-short/KIAA0148 is involved in subcellular localization of paxillin and actin cytoskeletal organization. Mol. Biol. Cell **12:**645–662.
36. **Mazaki, Y., S. Hashimoto, T. Tsujimura, M. Morishige, A. Hashimoto, K. Aritake, A. Yamada, J. M. Nam, H. Kiyonari, K. Nakao, and H. Sabe.** 2006. Neutrophil direction sensing and superoxide production linked by the GTPase-activating protein GIT2. Nat. Immunol. **7:**724–731.
37. **Menasche, G., S. Kliche, N. Bezman, and B. Schraven.** 2007. Regulation of T-cell antigen receptor-mediated inside-out signaling by cytosolic adapter proteins and Rap1 effector molecules. Immunol. Rev. **218:**82–91.
38. **Monks, C. R., B. A. Freiberg, H. Kupfer, N. Sciaky, and A. Kupfer.** 1998. Three-dimensional segregation of supramolecular activation clusters in T cells. Nature **395:**82–86.
39. **Nagy, A., J. Rossant, R. Nagy, W. Abramow-Newerly, and J. C. Roder.** 1993. Derivation of completely cell culture-derived mice from early-passage embryonic stem cells. Proc. Natl. Acad. Sci. USA **90:**8424–8428.
40. **Oh, W. K., J. C. Yoo, D. Jo, Y. H. Song, M. G. Kim, and D. Park.** 1997. Cloning of a SH3 domain-containing proline-rich protein, p85SPR, and its localization in focal adhesion. Biochem. Biophys. Res. Commun. **235:**794–798.
41. **Park, E., M. Na, J. Choi, S. Kim, J. R. Lee, J. Yoon, D. Park, M. Sheng, and E. Kim.** 2003. The Shank family of postsynaptic density proteins interacts with and promotes synaptic accumulation of the beta PIX guanine nucleotide exchange factor for Rac1 and Cdc42. J. Biol. Chem. **278:**19220–19229.
42. **Peterson, E. J., M. L. Woods, S. A. Dmowski, G. Derimanov, M. S. Jordan, J. N. Wu, P. S. Myung, Q. H. Liu, J. T. Pribila, B. D. Freedman, Y. Shimizu, and G. A. Koretzky.** 2001. Coupling of the TCR to integrin activation by Slap-130/Fyb. Science **293:**2263–2265.
43. **Phee, H., R. T. Abraham, and A. Weiss.** 2005. Dynamic recruitment of PAK1 to the immunological synapse is mediated by PIX independently of SLP-76 and Vav1. Nat. Immunol. **6:**608–617.
44. **Premont, R. T., A. Claing, N. Vitale, S. J. Perry, and R. J. Lefkowitz.** 2000. The GIT family of ADP-ribosylation factor GTPase-activating proteins. Functional diversity of GIT2 through alternative splicing. J. Biol. Chem. **275:**22373–22380.
45. **Premont, R. T., S. J. Perry, R. Schmalzigaug, J. T. Roseman, Y. Xing, and A. Claing.** 2004. The GIT/PIX complex: an oligomeric assembly of GIT family ARF GTPase-activating proteins and PIX family Rac1/Cdc42 guanine nucleotide exchange factors. Cell Signal. **16:**1001–1011.
46. **Reichardt, P., B. Dornbach, and M. Gunzer.** 2007. The molecular makeup and function of regulatory and effector synapses. Immunol. Rev. **218:**165–177.
47. **Rolink, A., F. Melchers, and J. Andersson.** 1996. The SCID but not the RAG-2 gene product is required for S mu-S epsilon heavy chain class switching. Immunity **5:**319–330.
48. **Rosenberger, G., A. Gal, and K. Kutsche.** 2005. AlphaPIX associates with calpain 4, the small subunit of calpain, and has a dual role in integrin-mediated cell spreading. J. Biol. Chem. **280:**6879–6889.
49. **Rosenberger, G., I. Jantke, A. Gal, and K. Kutsche.** 2003. Interaction of αPIX (ARHGEF6) with β-parvin (PARVB) suggests an involvement of αPIX in integrin-mediated signaling. Hum. Mol. Genet. **12:**155–167.
50. **Rosenberger, G., and K. Kutsche.** 2006. αPIX and βPIX and their role in focal adhesion formation. Eur. J. Cell Biol. **85:**265–274.
51. **Rozenblum, G. T., and M. Gimona.** 31 July 2007, posting date. Calponins: adaptable modular regulators of the actin cytoskeleton. Int. J. Biochem. Cell. Biol. doi:10.1016/j.biocel.2007.07.010.
52. **Schmits, R., T. M. Kundig, D. M. Baker, G. Shumaker, J. J. Simard, G. Duncan, A. Wakeham, A. Shahinian, A. van der Heiden, M. F. Bachmann, P. S. Ohashi, T. W. Mak, and D. D. Hickstein.** 1996. LFA-1-deficient mice show normal CTL responses to virus but fail to reject immunogenic tumor. J. Exp. Med. **183:**1415–1426.
53. **Shin, E. Y., K. S. Shin, C. S. Lee, K. N. Woo, S. H. Quan, N. K. Soung, Y. G. Kim, C. I. Cha, S. R. Kim, D. Park, G. M. Bokoch, and E. G. Kim.** 2002. Phosphorylation of p85 beta PIX, a Rac/Cdc42-specific guanine nucleotide exchange factor, via the Ras/ERK/PAK2 pathway is required for basic fibroblast growth factor-induced neurite outgrowth. J. Biol. Chem. **277:**44417–44430.
54. **Shin, E. Y., K. N. Woo, C. S. Lee, S. H. Koo, Y. G. Kim, W. J. Kim, C. D. Bae, S. I. Chang, and E. G. Kim.** 2004. Basic fibroblast growth factor stimulates activation of Rac1 through a p85 βPIX phosphorylation-dependent pathway. J. Biol. Chem. **279:**1994–2004.
55. **Tedford, K., L. Nitschke, I. Girkontaite, A. Charlesworth, G. Chan, V. Sakk, M. Barbacid, and K. D. Fischer.** 2001. Compensation between Vav-1 and Vav-2 in B cell development and antigen receptor signaling. Nat. Immunol. **2:**548–555.
56. **Togni, M., K. D. Swanson, S. Reimann, S. Kliche, A. C. Pearce, L. Simeoni, D. Reinhold, J. Wienands, B. G. Neel, B. Schraven, and A. Gerber.** 2005. Regulation of in vitro and in vivo immune functions by the cytosolic adaptor protein SKAP-HOM. Mol. Cell. Biol. **25:**8052–8063.
57. **Volinsky, N., A. Gantman, and D. Yablonski.** 2006. A Pak- and Pix-dependent branch of the SDF-1α signalling pathway mediates T cell chemotaxis across restrictive barriers. Biochem. J. **397:**213–222.
58. **Wang, H., F. E. McCann, J. D. Gordan, X. Wu, M. Raab, T. H. Malik, D. M. Davis, and C. E. Rudd.** 2004. ADAP-SLP-76 binding differentially regulates supramolecular activation cluster (SMAC) formation relative to T cell-APC conjugation. J. Exp. Med. **200:**1063–1074.
59. **Wang, H., E. Y. Moon, A. Azouz, X. Wu, A. Smith, H. Schneider, N. Hogg, and C. E. Rudd.** 2003. SKAP-55 regulates integrin adhesion and formation of T cell-APC conjugates. Nat. Immunol. **4:**366–374.
60. **Yoshii, S., M. Tanaka, Y. Otsuki, D. Y. Wang, R. J. Guo, Y. Zhu, R. Takeda, H. Hanai, E. Kaneko, and H. Sugimura.** 1999. αPIX nucleotide exchange factor is activated by interaction with phosphatidylinositol 3-kinase. Oncogene **18:**5680–5690.
61. **Za, L., C. Albertinazzi, S. Paris, M. Gagliani, C. Tacchetti, and I. de Curtis.** 2006. βPIX controls cell motility and neurite extension by regulating the distribution of GIT1. J. Cell Sci. **119:**2654–2666.